

Supporting Information

**Effects of Sulfation and Environment on Structure of Chondroitin Sulfate
Studied by Raman Optical Activity**

Václav Profant,^{*a} Christian Johannessen,^b Ewan W. Blanch,^c Petr Bour,^{*d} and Vladimír Baumruk^a

^aInstitute of Physics, Faculty of Mathematics and Physics, Charles University, Ke Karlovu 5, 121 16 Prague 2, Czech Republic

^bDepartment of Chemistry, University of Antwerp, Groenenborgerlaan 171, 2020 Antwerp, Belgium

^cSchool of Science, RMIT University, GPO Box 2476, Melbourne, VIC 3001, Australia

^dInstitute of Organic Chemistry and Biochemistry, Academy of Sciences, Flemingovo n. 2, 166 10 Prague 6, Czech Republic

* Corresponding authors,

V. P. Phone: +420 221911346. E-mail: profant@karlov.mff.cuni.cz,

P. B. Phone: +420 220183348, Email: bour@uochb.cas.cz.

Table S1. Vibrational analysis

Fig. S1. Singular value decomposition – CS forms

Fig. S2. Concentration dependence

Fig. S3. pH dependence

Fig. S4. Temperature dependence – Raman spectra of sample (1)

Fig. S5. Temperature dependence – SVD analysis of sample (4)

Fig. S6. Temperature dependence – SVD analysis of sample (1)

Fig. S7. Temperature dependence – ROA spectra

Table S1 Raman and ROA frequencies of chondroitin sulfate and its basic monosaccharide units.

C4S Raman	ROA	C6S Raman	ROA	GlcA Raman	GalNAc-4S Raman	GalNAc-6S Raman	Assignment
1648 (m) 1595 (w)		1648 (m) 1595 (w)		1595 (w, br)	1642 (m)	1641 (m)	Amide I (GalNAc)
1461 (w)		1461 (m)		1426 (-m)	1462 (m)	1455 (m)	COO asymmetric deformation (GlcA)
1415 (s)	1425 (-m)	1414 (s)		1416 (s)			CH ₂ deformation (GalNAc)
1373 (s)	1377 (+s)	1380 (s)	1379 (+s)	1360 (+s) / 1335 (-m)	1362 (s)	1380 (s)	COO symmetric deformation (GlcA)
1343 (s)	1357 (+s) / 1332 (-m)	1343 (s)		1298 (-m)	1302 (m)	1331 (s)	CH ₃ symmetric deformation (GalNAc)
1270 (m, br) 1239 (sh)	1300 (-m) 1238 (+m)	1262 (+m)	1274 (m)	1269 (+s)	1240 (w)	1271 (s)	CH bending deformations (GlcA)
1205 (w) 1159 (m)		1206 (w) 1162 (m)		1165 (+m)	1204 (w) 1152 (m)	1225 (sh)	Amide III (GalNAc)
1135 (sh)	1133 (-s)	1135 (w)	1124 (sh)	1142 (-w)	1118 (s)	1141 (m)	C(5)H bending deformation (GlcA)
1117 (-s)		1098 (w)		1107 (-s) / 1089 (+s)		1127 (w) 1094 (w)	OSO ₃ asymmetric stretch (partially)
1081 (s)	1089 (+s) / 1073 (-m)	1065 (vs)		1061 (s)	1082 (vs)	1065 (vs)	OSO ₃ symmetric stretch
1052 (s)	1052 (-m)	1035 (sh)		1040 (s)	1050 (s)	1032 (m)	
1029 (sh)	1027 (+w)	1007 (-m)	999 (w)	1007 (+m)	1016 (s)	1016 (s)	
978 (m)	973 (+m)	983 (sh)	983 (+m)			998 (s)	C-O-S stretch, partly COH and CH deformations
940 (m)	913(+w)/937(-m)	940 (m)	913(+w)/939 (-m)		973 (s)	980 (sh)	
891 (w)	881 (+w)	888 (m)	884 (w)		895 (w)	881 (sh)	
862 (m)	865 (+w)	864 (w)	831 (m)		864 (m)	885 (m)	
803 (w)	818 (+w)				830 (w)	832 (sh)	
725 (m)	764 (-w)	725 (w)	764 (+w)		801 (w)	803 (m)	C-O-S deformations + skeletal modes
641 (w, br)	661 (-m)	661 (-m)		661 (-m)		760 (s)	
593 (w, br) 552 (w, br)	603 (-m) 545 (+m)	581 (m)	604 (-m, br)	622 (w)	631 (m)	621 (m)	
500 (-w)	500 (-w)	532 (+m)		576 (m)	603 (m)	591 (m)	
465 (+m)	465 (+m)	469 (sh)	504 (-w)	517 (w)	562 (m)	533 (m)	
420 (w, br)	423 (-w)	416 (m)	427 (-w)	460 (s)	436 (sh)	495 (w)	
377 (m)	397 (+vs)	376 (w)	387 (+m, br)	417 (s)	416 (m)	441 (m)	
339 (m)	343 (+w)	335 (w, br)	319 (-m)	343 (m)	368 (w)	361 (w)	skeletal modes
293 (m)	306 (-sh)	281 (m, br)	251 (-m, br)	290 (sh)	323 (w)	315 (w)	
	279 (-s, br)				271 (w)	292 (w)	
							C4S, chondroitin 4-sulfate; C6S, chondroitin 6-sulfate; GalNAc-4S, N-acetyl-galactosamine 4-sulfate; GalNAc-6S, N-acetyl-galactosamine 6-sulfate; GlcA, D-glucuronic acid; (s), strong; (m), medium; (w), weak; (sh), shoulder; (br), broad; (vs), very strong; (+), positive; (-), negative; ... / ..., couplet.

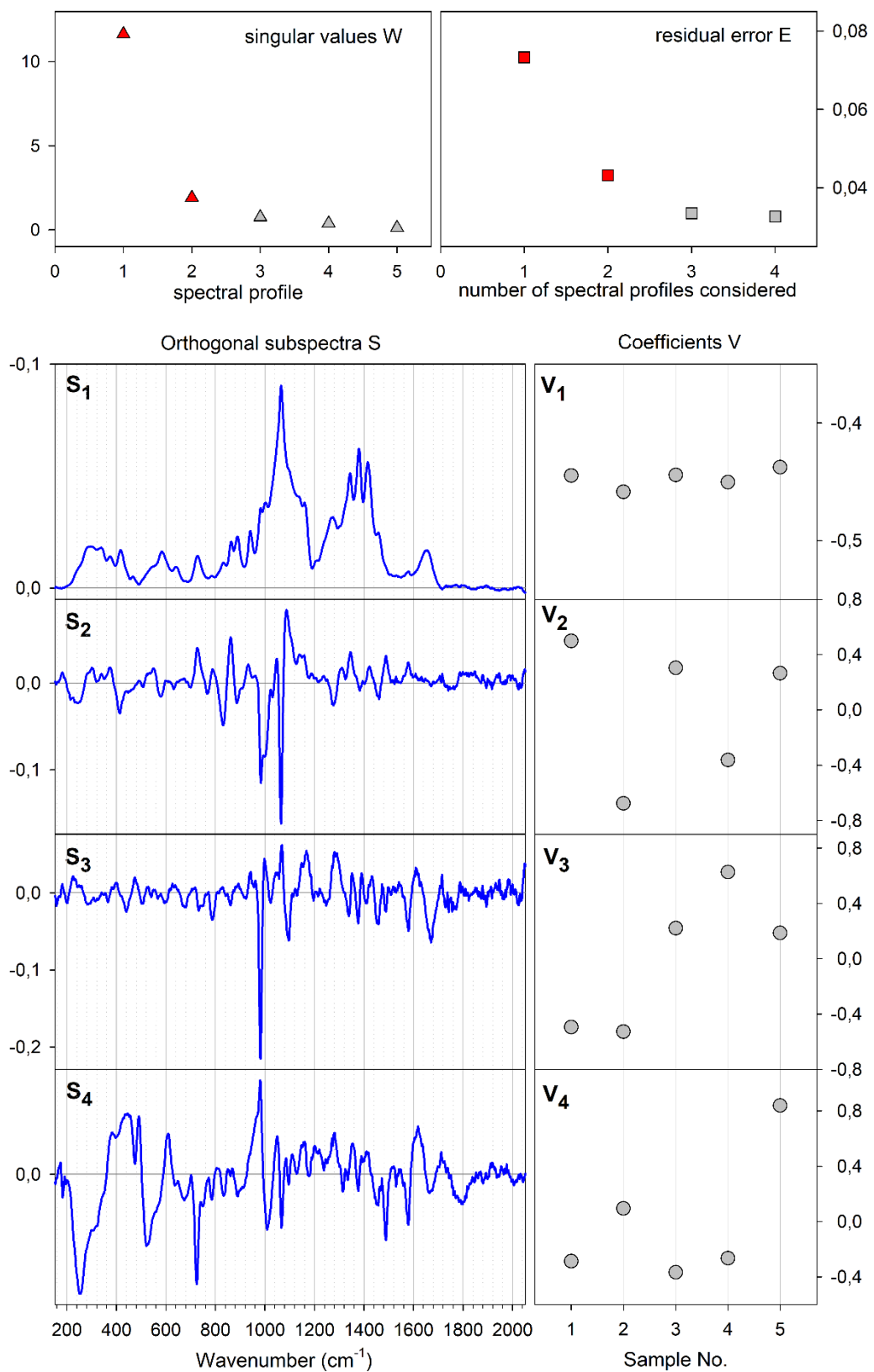


Fig. S1 The factor analysis of Raman spectra of different CS samples (see Table 1 for identification).

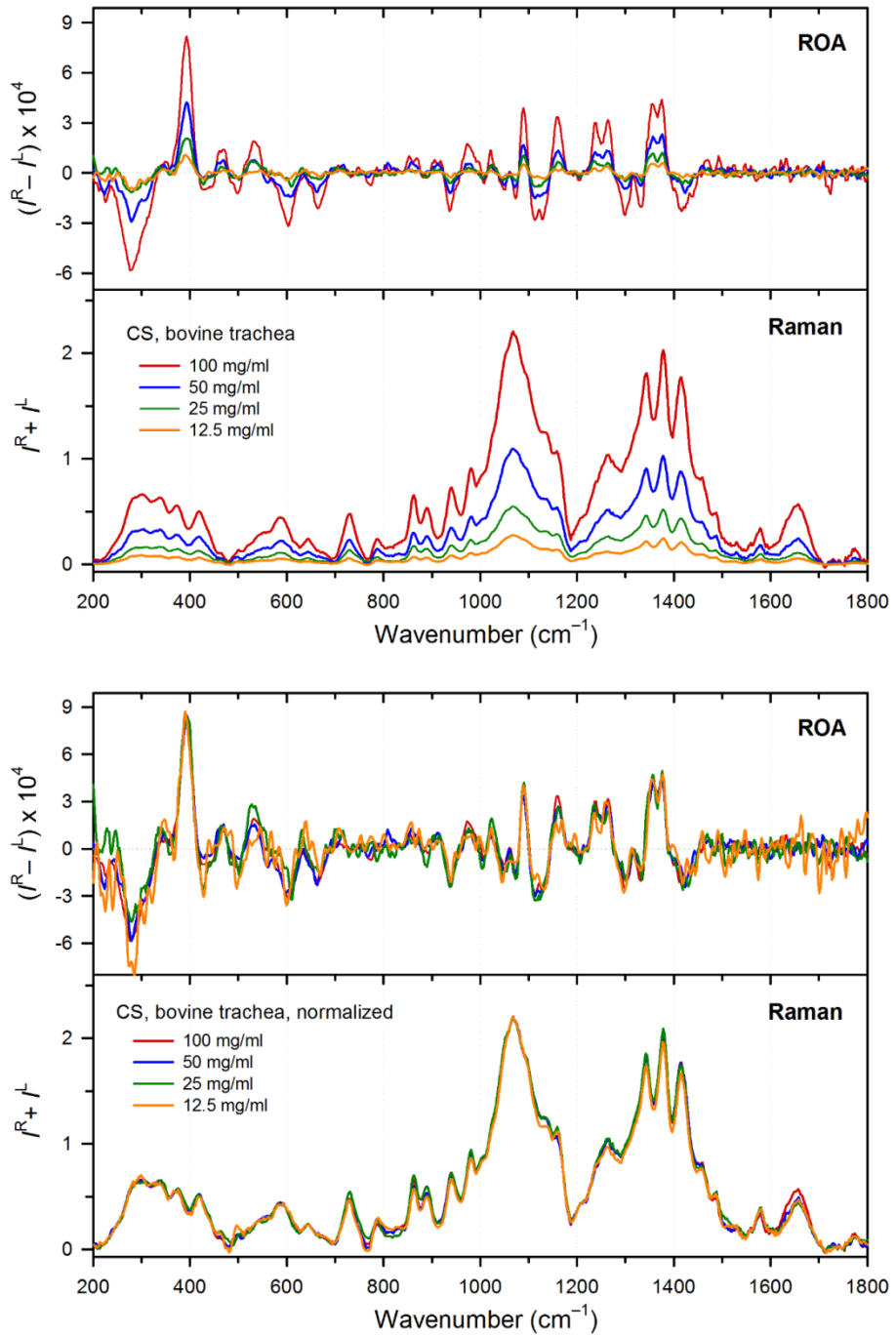


Fig. S2 Raman and ROA spectra of CS sodium salt from bovine trachea (1) at various concentrations. The upper panels show spectra normalized on the same accumulation time; the lower panels display spectra normalized on the same integral intensity (using Raman spectrum in $500 - 1700 \text{ cm}^{-1}$ interval).

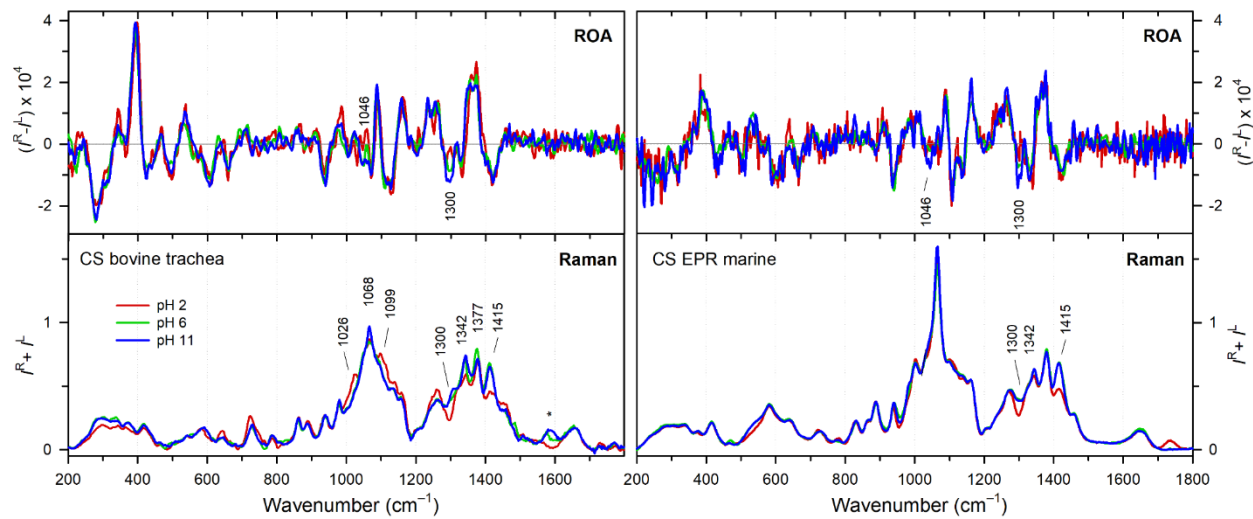


Fig. S3 Raman and ROA spectra of CS from bovine trachea (left) and CS EPR marine (right) at neutral (pH 6, green), basic (pH 11, blue), and acidic (pH 2, red) environment. The major changes in spectra are labelled. The band at 1590 cm^{-1} corresponding to sample's impurities is marked by asterisk.

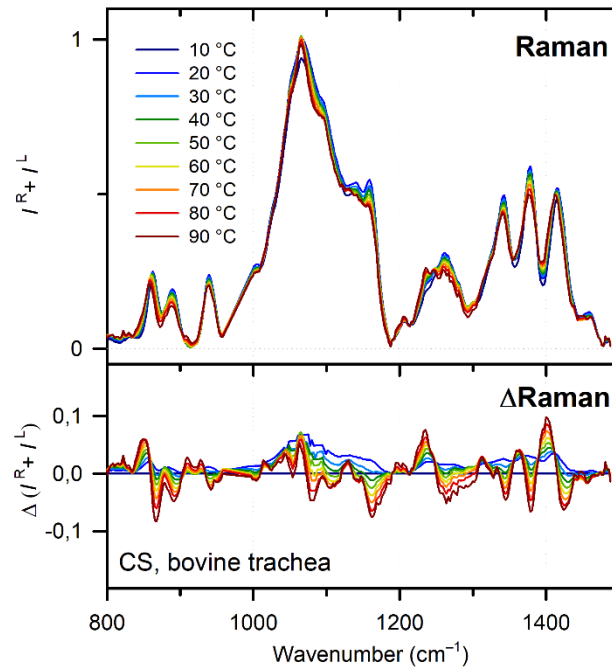


Fig. S4 Raman and difference (vs. 10°C) Raman spectra of CS from bovine trachea measured at various temperatures.

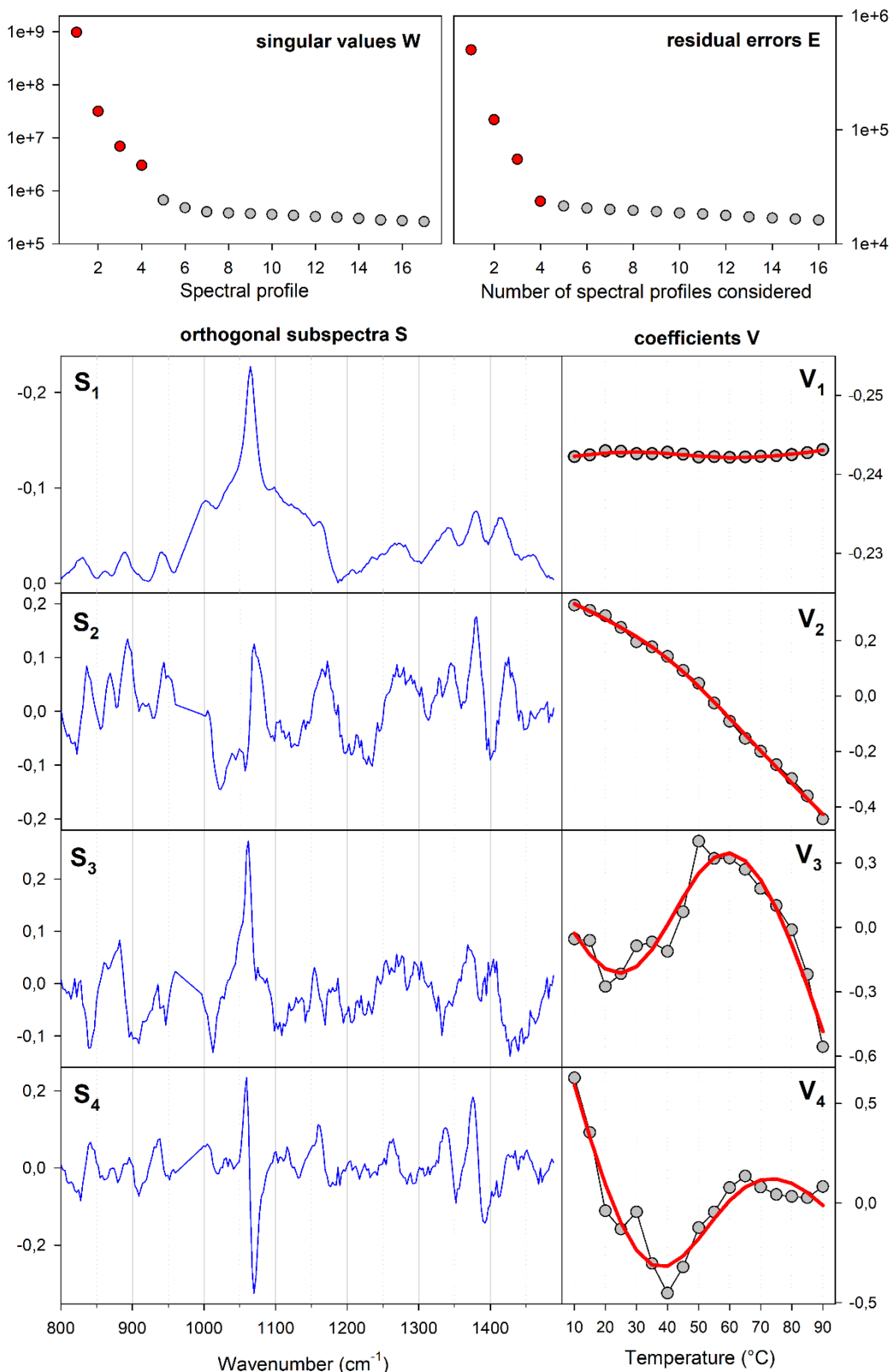


Fig. S5: The factor analysis of Raman spectra temperature dependence of CS EPR marine. Result of the one-step transition fit is shown by red lines.

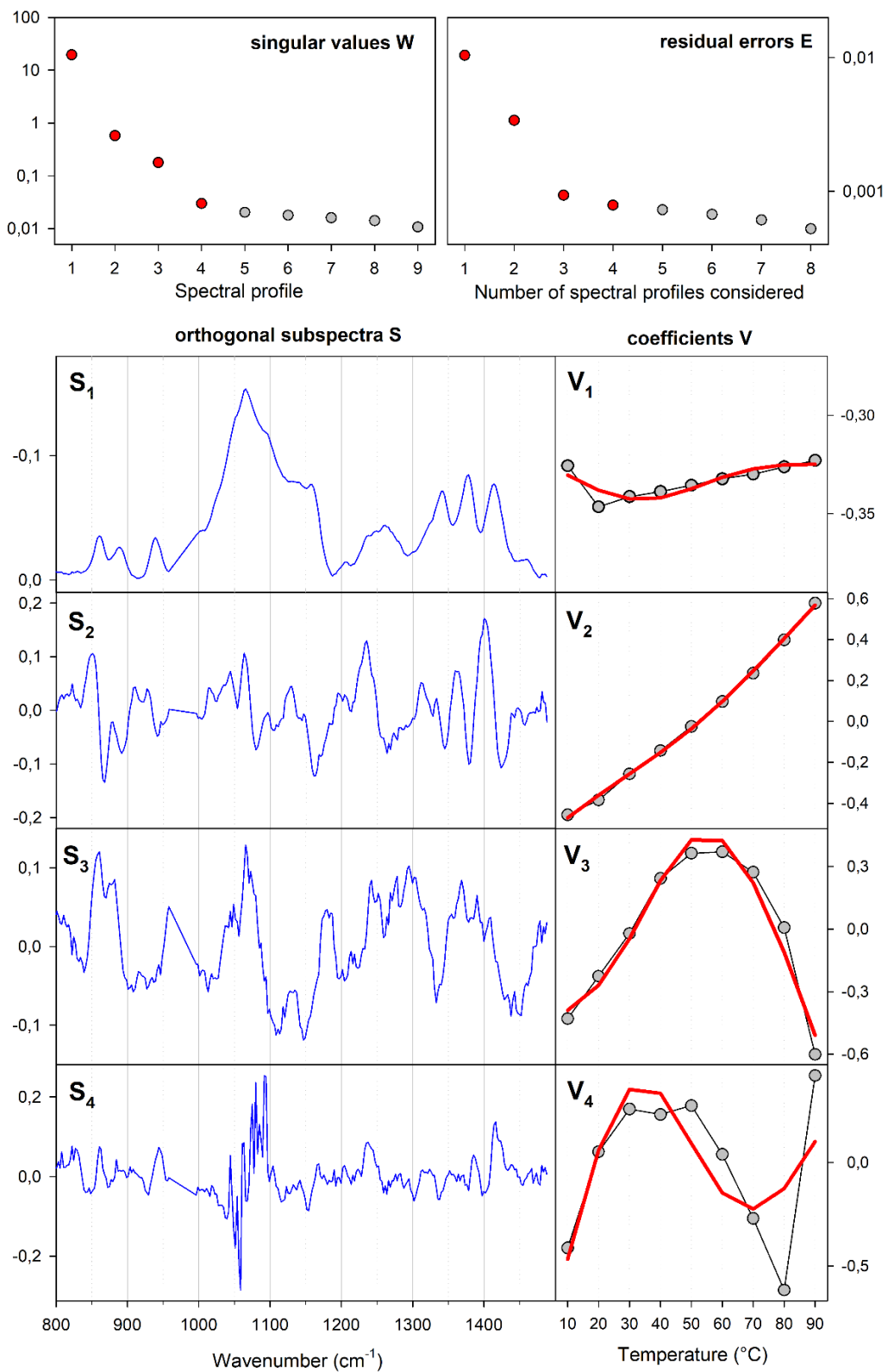


Fig. S6 The factor analysis of Raman spectra temperature dependence of CS bovine trachea. Result of the one-step transition fit is shown by red lines.

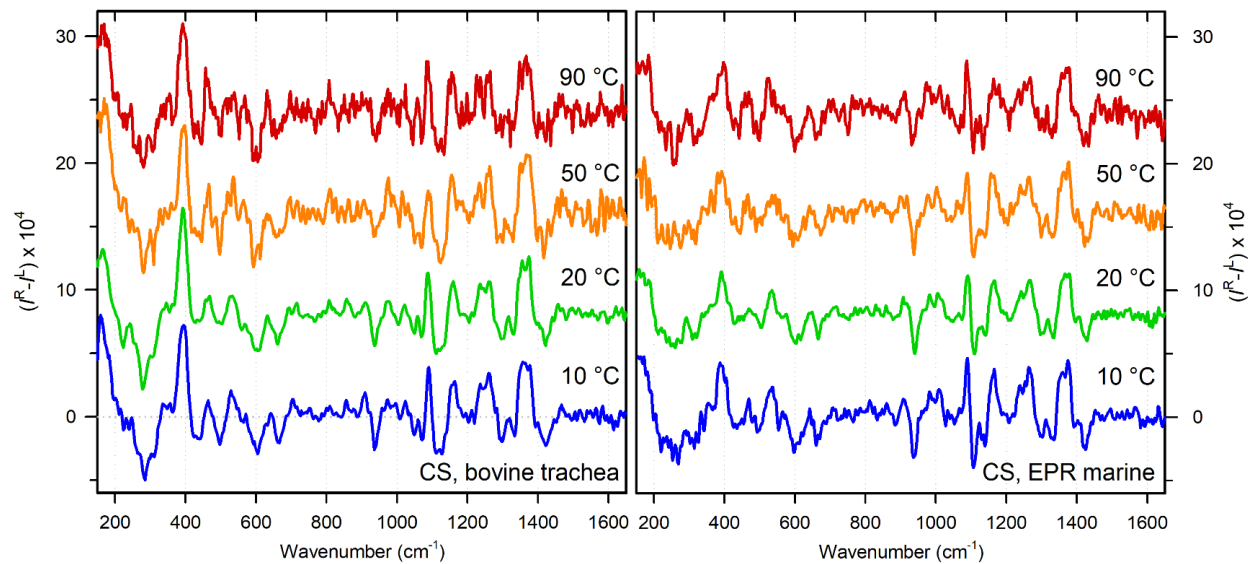


Fig. S7 ROA spectra of CS from bovine trachea (left) and CS EPR marine (right) at various temperatures. The spectra belong to the Raman spectra in Fig. S4 and Fig. 8 measured at each corresponding temperature. The same factor was used for normalization of both Raman and ROA spectra.